

[CONTRIBUTION FROM THE DEPARTMENT OF CHEMISTRY, UNIVERSITY OF WASHINGTON]

A New Multilayer Isotherm with Reference to Entropy^{1,2}By W. M. CHAMPION³ AND G. D. HALSEY, JR.

RECEIVED SEPTEMBER 14, 1953

An earlier isotherm has been modified to take account of variations in entropy of adsorption. Instead of using a step-function for adsorption on sites of a given energy χ the lateral interaction w has been made a function of χ and the equations of Hill used to calculate coverage. Graphical means are used to calculate thermodynamic functions for a number of distributions of χ . These functions are similar to experimental results.

Introduction.—In a previous paper⁴ there was developed a multilayer isotherm adequate to reproduce isotherms at a single temperature. The entropy was assumed to be that of the bulk phase, and so the temperature dependence of the isotherm was fixed. Numerous investigations⁵ have shown that the entropy is variable. In this paper we refine our model to include variations in the entropy of adsorption.

The Model.—The model is similar to that of the earlier paper except that any distribution function for energy of adsorption can be used and the step-function adsorption isotherm is replaced. Instead, the equations due to Hill⁶ and used previously by us⁷ for multilayer adsorption with interaction are used

$$p/p_0 = \frac{(\theta_n - \theta_{n+1})/(\theta_{n-1} - \theta_n)}{\theta = \sum \theta_n} \times \exp\{\chi_n/kT + 2\theta w/kT\} \quad (1)$$

Here p/p_0 is the partial pressure, θ_n the coverage in the n 'th layer on sites of energy χ_n (negative for

heat evolved), w the lateral interaction, and θ total coverage. Formally these n equations must be solved simultaneously, but we have found⁴ that if the energy decays rapidly with n only one layer fills at a time over a given strength site. Thus $\theta_{n-1} \approx 1$ and $\theta_{n+1} \approx 0$, which makes the computation of $\theta\chi$, the coverage on sites of energy χ , very easy.

One assumption that is retained from the earlier paper is that sites of equal energy are grouped together, and not mixed with other energies. For this reason, we can treat the sites of one energy independently, and use equation 1. The problem is solved graphically, and the coverage in each layer θ_n is represented on a rectangular graph. This is shown for the first two layers in Fig. 1. The strong sites are at the right and the non-linear scale gives the relative abundance of sites of varying energy. Lines running across the graph give the coverage on the various sites at a given pressure.

The Interaction Energy.—The value of $-w_0/kT$ in the bulk phase is about 5 at the boiling point. For this value of $-w/kT$ equation 1 is almost a step function. If the surface lattice of the adsorbent exactly fitted the bulk phase, $-w/kT$ would always be large and the entropy of adsorption relative to the bulk phase would be near zero. However, if the lattices were incompatible $-w/kT$ might become zero or even repulsive if the surface forces were strong enough to change the arrangement of atoms favorable for lateral interaction. This is because the largest value of χ is obtained when the adsorbed atom is located in a best position relative to the lattice of the solid. In general, the next such best position will not be located at exactly the right distance for the realization of w_0 , unless the lattices of the adsorbent and adsorbate are exactly the same. Only at large distances from the surface or on weak sites the interaction energy would rise to the bulk value of $-w_0/kT$.

The simplest equation having these properties is

$$-w/kT = (-w_0/kT) - a(-\chi/kT) \quad (2)$$

When the incompatibility factor $a = 0$, the interaction energy is always that of the bulk phase. As a increases to unity the lattices become more and more incompatible. We have not considered values of a greater than unity because it emerges that a value of unity produces a discontinuity in the isotherm; larger values cause the sites with small values of $(-\chi/kT)$ to fill first. The form of 2 used here is

$$-w/kT = 5 - a(-\chi/kT) \quad (3)$$

for positive values of $(-w/kT)$. Instead of the repulsive values predicted by 3 the value zero for w/kT is substituted. Because of the graphical

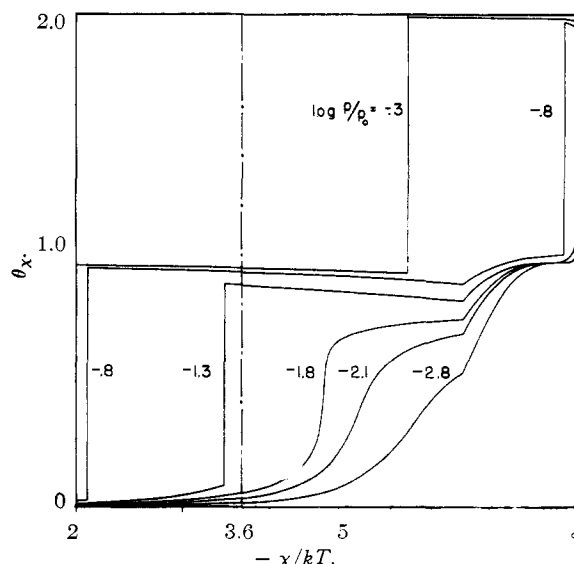


Fig. 1.—A plot of θ_χ vs. $-\chi/kT$ for $a = 5/8$ and $-\chi_m/kT = 4$ for the first and second layers.

(1) This research was supported by Contract AF19(604)-247 with the Air Force Cambridge Research Center.

(2) Presented at the 124th National Meeting of the Am. Chem. Soc., Chicago, Ill., Sept. 6-11, 1953.

(3) Presented in partial fulfillment of the requirements for the degree of Doctor of Philosophy.

(4) G. D. Halsey, Jr., *This Journal*, **73**, 2693 (1951).

(5) See for example T. L. Hill, P. H. Emmett and L. G. Joyner, *ibid.*, **73**, 5102 (1951).

(6) T. L. Hill, *J. Chem. Phys.*, **15**, 767 (1947).

(7) W. M. Champion and G. D. Halsey, Jr., *J. Phys. Chem.*, **57**, 646 (1953).

nature of the computation any other relationship between χ and w could be used.

It is necessary to adjust the zero of χ in equation 1 to make χ the energy relative to the bulk phase; the total energy of a completed monolayer is $\chi + w$. When $w = w_0$, the bulk phase value, χ must equal $-w_0$ to make the total energy zero with respect to the bulk phase. For this reason $(-w_0/kT)$ must be added to the exponent in 1 to make $\chi = 0$ for the bulk phase. The final form of the isotherm used to calculate the coverage θ_χ on sites of energy χ is then

$$p/p_0 = (\theta_\chi/1 - \theta_\chi) \exp\{-2\theta_\chi(-w/kT) - (-\chi/kT) + 5\} \quad (4)$$

When $w = w_0$ and $\chi = 0$, this equation agrees with the properties of the bulk phase.

Calculation of the $(-\chi/kT)$ Scale.—The rectangular plate that represents the first monolayer must be given a non-linear scale that represents the distribution function for $(-\chi/kT)$. If a linear scale α running from zero at the right to unity at the left is defined, then in terms of the distribution function $N(-\chi/kT)$

$$\alpha = \int_{(-\chi/kT)}^{\infty} N(-\chi/kT) d\chi / \int_{-\infty}^{\infty} N(-\chi/kT) d\chi \quad (5)$$

For the particular case of the exponential distribution function

$$N(-\chi/kT) = C \exp\{-(-\chi/kT)/(-\chi_m/kT)\} \quad (6)$$

with a cut-off at $(-\chi_0/kT)$

$$\alpha = \exp\{(-\chi_0/kT) - (-\chi/kT)/\chi_m/kT\} \quad (7)$$

The scale in Fig. 1 was laid out using 7 with $(-\chi_m/kT) = 4$ and $(-\chi_0/kT) = 2.044$. The scale for the n 'th layer is found directly from the first layer by dividing by n^3 .

Calculation of the Isotherm.—For a given value of p/p_0 , values of θ_χ are plotted as a function of $-\chi/kT$. The area under this curve is then determined, using a planimeter. This area, divided by the area of the whole monolayer, gives θ_1 , the coverage in the first layer. A similar procedure gives θ_2 , the coverage in the second layer. When the critical value of the interaction energy is reached $(-w/kT = 2)$, discontinuities in the θ_χ vs. $-\chi/kT$ curves appear. For the third and higher layers, the adsorption is almost entirely step-wise, and it is no longer necessary to integrate graphically. The sum of θ_n gives θ as a function of p/p_0 , and thus the isotherm. (For the case of the exponential distribution we have retained the notation $\theta_{0.6}$ for $\exp\{-\chi_0/\chi_m\} = 0.6$, etc.)

Calculation of the Integral Entropy.—The molar entropy of adsorption on sites of energy χ can be written⁵

$$S_\chi/k = \ln B!/(B - N_\chi)!N_\chi! \quad (8)$$

where B is the number of sites and N_χ the number of adsorbed molecules.

The molar integral entropy of adsorption over all sites equals

$$S/k = \int N_\chi \theta_\chi (S_\chi/k) d\chi / \int N_\chi \theta_\chi d\chi \quad (9)$$

The quantity that must be integrated over all values of χ is thus $\theta_\chi S_\chi$. If we use Stirling's

approximation and write $\theta = N_\chi/B$, we find from equation 8

$$\theta_\chi (S_\chi/k) = -\theta_\chi \ln \theta_\chi - (1 - \theta_\chi) \ln (1 - \theta_\chi) \quad (10)$$

Figure 2 shows this quantity plotted as a function of $-\chi/kT$ for various values of p/p_0 . The parameters are the same as in Fig. 1. Use of the planimeter yields the numerator in equation 9; only contributions from the first two layers are important. The denominator is the isotherm.

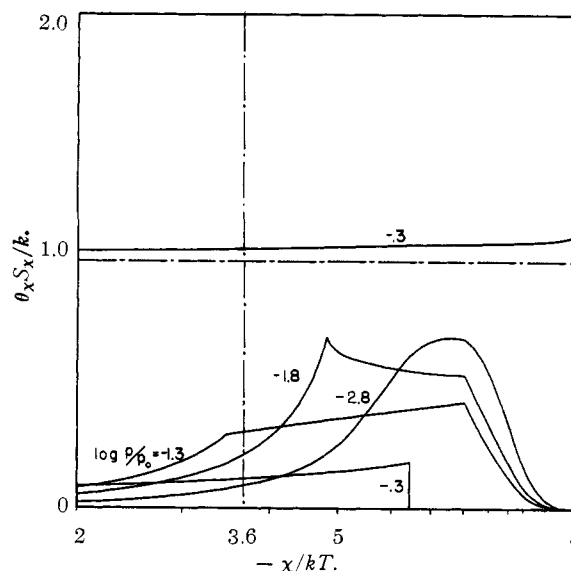


Fig. 2.—A plot of $\theta_\chi S_\chi/k$ vs. $-\chi/kT$ for $a = 5/8$ and $-\chi_m/kT = 4$ for the first and second layers.

For the special case of the exponential isotherm the limiting value of S can be calculated. Near $\theta = 0$ interaction can be ignored because $w = 0$ for the strongest sites. For this case the isotherm becomes⁸

$$\theta = \exp\{\chi_0/\chi_m\} (p/p_0)^{-kT/\chi_m} (-kT/\chi_m) \pi \csc \pi (-kT/\chi_m) \quad (11)$$

This expression yields a differential entropy that is independent of θ

$$\bar{S}/k = (-\chi_m/kT) - \pi \cot \pi (-kT/\chi_m) \quad (12)$$

At zero coverage the differential entropy equals the integral entropy. For any distribution function with finite limits, S approaches infinity as θ approaches zero.

Calculation of the Differential Entropy.—The differential entropy is related to the integral entropy by the expression⁵

$$\bar{S} = S + \theta (\partial S / \partial \theta) \quad (13)$$

Equation 9 can be written

$$S = [\int S_\chi \theta_\chi N_\chi d\chi] / \theta \quad (14)$$

whence

$$\bar{S} = (\partial / \partial \theta) [\int S_\chi \theta_\chi N_\chi d\chi] \quad (15)$$

$$= [\partial (\int S_\chi \theta_\chi) / \partial (\ln p/p_0) N_\chi d\chi] / \partial \theta \partial \ln p/p_0 \quad (16)$$

The integral in the numerator can be evaluated using 4 and 10

$$I_1 \equiv - \int \{ [\ln(\theta_\chi/1 - \theta_\chi)] [\theta_\chi(1 - \theta_\chi)] / [1 - 2(-w/kT)\theta_\chi(1 - \theta_\chi)] \} N_\chi d\chi \quad (17)$$

(8) G. D. Halsey, Jr., *Advances in Catalysis*, IV, 259 (1952).

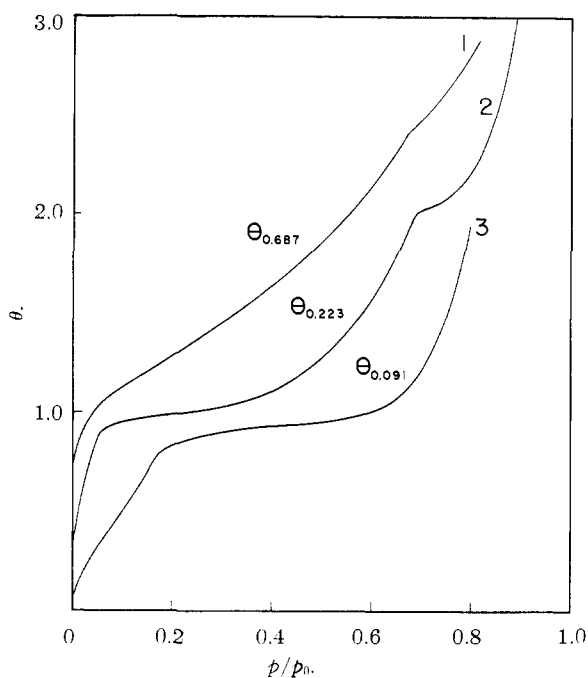


Fig. 3.—Calculated isotherms: for curve 1, $a = 1/2$, $-\chi_m/kT = 16$; for curve 2, $a = 1/2$, $-\chi_m/kT = 4$; for curve 3, $a = 5/8$, $-\chi_m/kT = 2$.

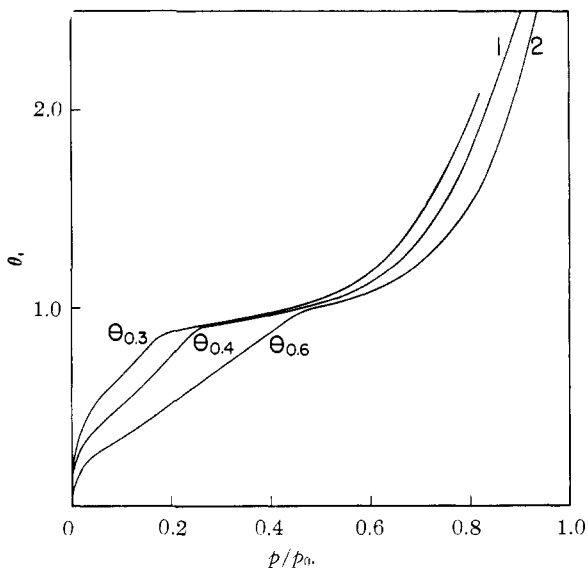


Fig. 4.—Calculated isotherms for $a = 5/8$ and $-\chi_m/kT = 4$.

This expression can be integrated graphically. Similarly a second integral can be written for part of the quantity

$$I_2 \equiv \int \{\theta_x(1 - \theta_x)/[1 - 2\omega\theta_x(1 - \theta_x)]N_x\} dx \quad (18)$$

This integral does not contain the contribution due to the discontinuities in θ_x . This can be shown to be

$$D = (1 - 2\theta_L)\partial\alpha(\theta_x = 1/2)/\partial \ln p/p_0 \quad (19)$$

for each layer. Here θ_L is the lower end of the discontinuity and the derivative is the rate of move-

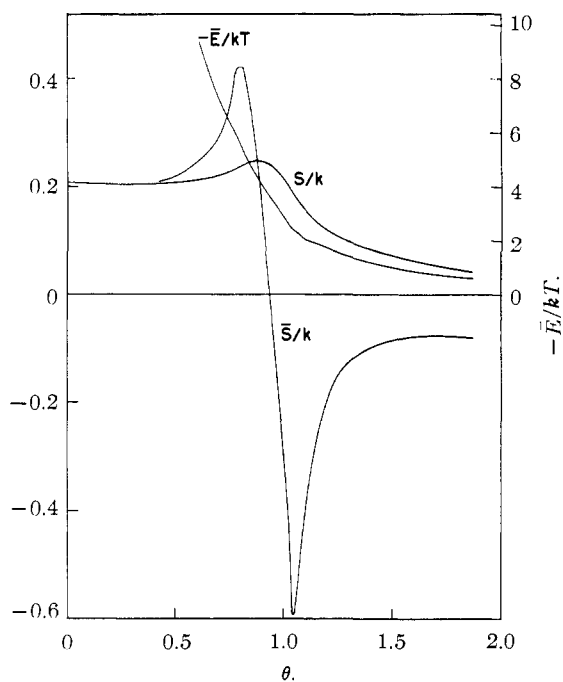


Fig. 5.—The heat and entropy curves for isotherm 1 in Fig. 3: $a = 1/2$, $-\chi_m/kT = 16$, $-\chi_0/kT = 6$.

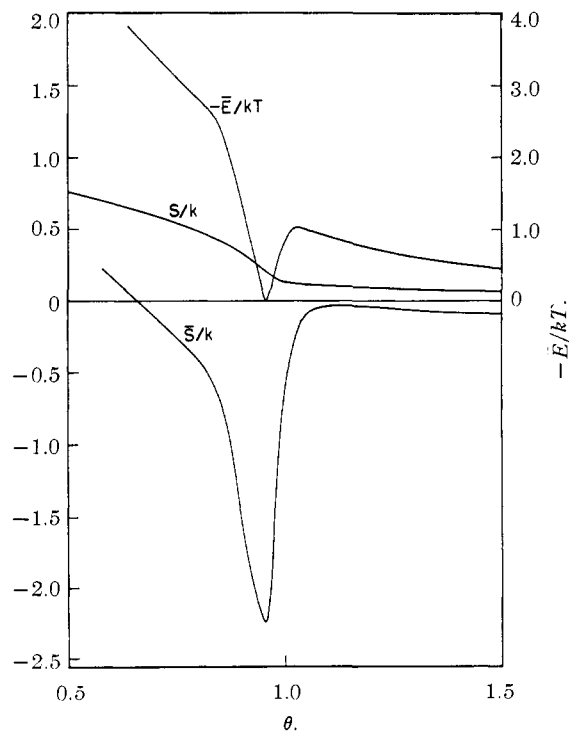


Fig. 6.—The heat and entropy curves for isotherm 2 in Fig. 3: $a = 1/2$, $-\chi_m/kT = 4$, $-\chi_0/kT = 6$.

ment of the "riser" of the step with $\ln p/p_0$. The differential entropy then equals

$$\bar{S}/k = I_1/(I_2 + D) \quad (20)$$

This formula was used to check a few of the differential entropies obtained directly from the calculated integral entropies by the use of 13.

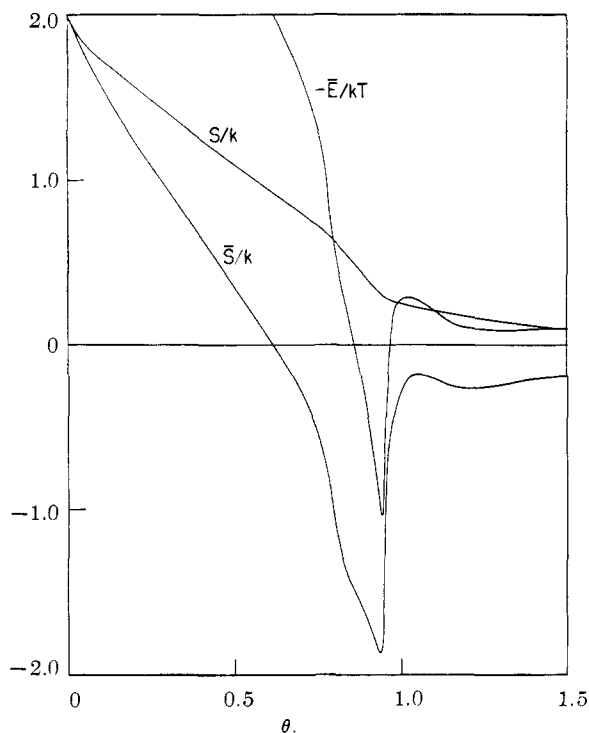


Fig. 7.—The heat and entropy curves for isotherm 3 in Fig. 3: $a = 5/8$, $-\chi_m/kT = 2$, $-\chi_0/kT = 4.8$.

Calculation of the Energies.—The integral energy per molecule relative to the bulk phase on sites of uniform energy χ is given by the expression

$$-E_{\chi}/kT = -\chi/kT - 5 + (-w/kT)\theta_{\chi} \quad (21)$$

Analogous to 9 the integral energy over all sites is then

$$E = \int E_{\chi}\theta_{\chi}N_{\chi}d\chi/\theta \quad (22)$$

The differential energy of adsorption

$$\bar{E} = E + \theta(\partial E/\partial\theta)$$

is given by an expression analogous to 15

$$\bar{E} = (\partial/\partial\theta)[\int E_{\chi}\theta_{\chi}N_{\chi}d\chi] \quad (23)$$

It emerges that the value so calculated is equal to the energy calculated with the expression

$$-\bar{E}/kT = -\bar{S}/k - \log p/p_0 \quad (24)$$

This equation corresponds to the thermodynamic equation $H = \bar{F} + T\bar{S}$, which shows $\bar{H} = \bar{E}$.

Calculated Examples.—In Figs. 3 and 4, six isotherms calculated by the method of this paper are presented. Various exponential distributions were assumed, and the results are quite similar to the isotherms calculated with the simpler model.⁴

Curve 1 in Fig. 3 is representative of the usual type of experimental isotherm, and curve 2 is typical of the isotherms given by a nearly uniform surface.⁹

The third isotherm of Fig. 3 and the isotherms of Fig. 4 are similar to those found by Orr¹⁰ for the adsorption of A, N₂ and O₂ on KCl.

Thermodynamic functions for the first isotherm, Fig. 3, are shown in Fig. 5. The distribution function chosen corresponds to a strongly adsorbing,

(9) R. A. Beebe, J. Biscoe, W. R. Smith and C. B. Wendell, *THIS JOURNAL*, **69**, 95 (1947).

(10) W. J. C. Orr, *Proc. Roy. Soc. (London)*, **A173**, 349 (1939).

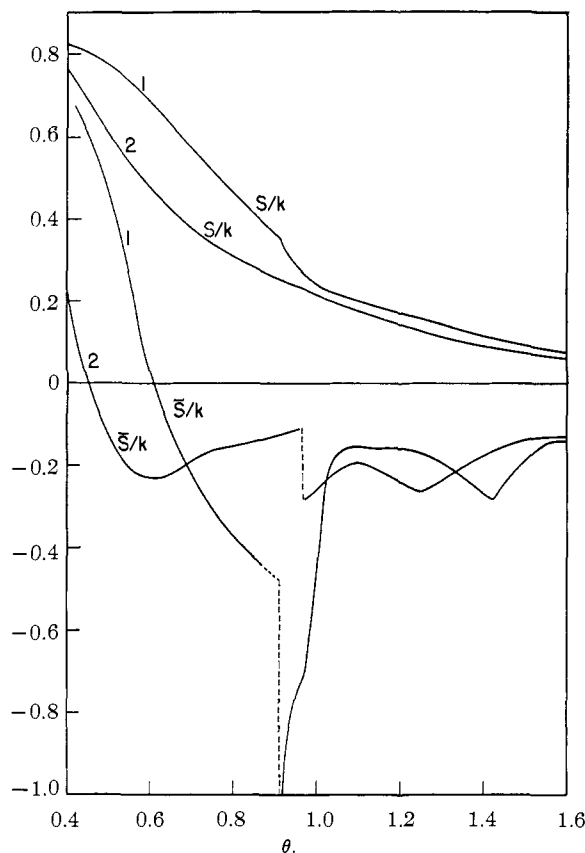


Fig. 8.—The entropy curves for isotherms 1 and 2 in Fig. 4: for curve 1, $a = 5/8$, $-\chi_m/kT = 4$, $-\chi_0/kT = 3.66$; for curve 2, $a = 5/8$, $-\chi_m/kT = 4$, $-\chi_0/kT = 2.044$.

strongly heterogeneous surface. The differential energy $-\bar{E}/kT$ descends rapidly with a barely perceptible bumpiness near $\theta = 1$. \bar{S}/k shows the characteristic minimum⁴ near $\theta = 1$. S and \bar{S} show interesting maxima as they rise from the rather artificial limit imposed by equation 12. The thermodynamic functions for the second isotherm of Fig. 3 are shown in Fig. 6. The energy $-\bar{E}/kT$ has developed the characteristic minimum⁹ associated with a more nearly uniform surface. The isotherm shows a bump at $\theta = 2$, also characteristic of a uniform surface.¹¹ The depth of the minimum in \bar{S} has increased. These calculations were not taken below $\theta = 1/2$; it is not clear at this value of θ that \bar{S} is approaching its limit. S and \bar{S} no longer exhibit maxima.

In Fig. 7, corresponding to the third isotherm, the a has been increased and the modulus ($-\chi_m/kT$) further decreased. Negative values of $-\bar{E}/kT$ are reached near $\theta = 1$. The upper limit of S and \bar{S} is now much larger; the total range of \bar{S} is about 8 e.u. Milder fluctuations in S in the second layer are noticeable. In the isotherms of Fig. 4, only the value of the cut-off is varied. For isotherms numbered 1 and 2 the cut-off is beyond the critical value of $-w/kT = 2$. The entropies for these two are shown in Fig. 8. For isotherm 1, \bar{S} shows a large minimum, with a discontinuity. This discontinuity is caused

(11) M. H. Polley, W. D. Schaeffer and W. R. Smith, *J. Phys. Chem.*, **57**, 469 (1953).

by the abrupt termination of the step adsorption in the first layer by the sharp cut-off, and it has no physical significance. The cut-off for isotherm 2 is smaller and \bar{S} has lost its deep minimum at $\theta = 1$.

Discussion.—Because of the exponential distribution, the upper limit of $-\bar{E}/kT$ has the unrealistic value infinity for the examples treated here. We refrained from using an upper cut-off, which would have given $-\bar{E}/kT$ a finite limit, in order to keep the number of parameters down. None of the integral entropies has a minimum near the monolayer⁵ because we have kept the entropy of binding to the surface equal to that in the bulk phase. This

restriction is easily removed⁸ (with still another parameter) and the observed minimum in S could be reproduced.

As yet, we are unable to make any generalizations connecting the limited number of parameters and the thermodynamic functions that result; for instance the negative value of $-\bar{E}/kT$ in Fig. 7 came as a complete surprise. If anything, this difficulty demonstrates the folly of making deductions about the model for adsorption from qualitative examination of, and *ad hoc* calculations on, experimental heats and entropies.

SEATTLE, WASHINGTON

[CONTRIBUTION FROM THE MINERALS THERMODYNAMICS BRANCH, REGION III, BUREAU OF MINES, UNITED STATES DEPARTMENT OF THE INTERIOR]

Heats of Formation of Tantalum, Niobium and Zirconium Oxides, and Tantalum Carbide

BY GEORGE L. HUMPHREY

RECEIVED OCTOBER 17, 1953

The heats of formation of tantalum pentoxide, niobium (columbium) pentoxide, zirconium dioxide and tantalum carbide were measured by combustion calorimetry. The results are, respectively, -488.8 ± 0.5 , -455.2 ± 0.6 , -261.5 ± 0.2 , and -38.5 ± 0.6 kcal./mole at 298.16°K. Corresponding free energy values were calculated.

The present availability of zirconium almost completely free of hafnium and of substantially pure tantalum and niobium (columbium) made it desirable that new determinations be obtained of the heats of formation of the oxides of these metals. This was accomplished through combustion calorimetry and the results are reported in this paper, together with determinations of the heats of combustion and formation of substantially pure tantalum carbide.

Materials and Method.—The tantalum metal was obtained from Fansteel Metallurgical Corp. in the form of half-inch bar stock. Spectrographic analysis¹ showed 0.08% niobium, 0.01% silicon, 0.01% iron and 0.005% titanium, indicating a purity of 99.89%. The increase in mass on complete conversion to oxide agreed with the result calculated from this analysis to within 0.02%. Very thin lathe-turnings, cut from the interior of the bar with a Carboloy tool were used in the measurements.

The niobium metal also was a Fansteel Metallurgical Corp. product. It was received in 0.005-inch thick sheets that were cut into narrow strips for use in the measurements. Spectrographic analysis¹ showed 0.20% tantalum, 0.05% tungsten, less than 0.01% each of silicon, molybdenum, iron and boron, less than 0.005% each of aluminum, manganese, nickel and zirconium, less than 0.003% titanium and 0.001% copper. The indicated purity, therefore, is about 99.69%.

The zirconium metal was furnished by the Albany (Oregon) Station of the Bureau of Mines, along with the results of chemical and spectrographic analyses. The impurities are less than 0.1% hafnium, 0.09% iron, 0.053% chlorine, 0.03% carbon, 0.011% magnesium, 0.009% aluminum, 0.009% lead, 0.007% nitrogen, 0.006% titanium, 0.002% chromium, 0.002% manganese, 0.001% silicon, 0.001% copper and less than 0.001% each of boron, molybdenum, nickel and tin. The indicated purity thus is 99.67%. Part of the metal was in the form of vacuum purified sponge, which was used as received, and part in the form of a machined bar, from which very thin lathe-turnings (cut from the interior with a Carboloy tool) were taken for the measurements.

The tantalum carbide was obtained, in powder form,

(1) This analysis was conducted by George M. Gordon, Division of Mineral Technology, University of California.

from Fansteel Metallurgical Corp. Spectrographic analysis¹ showed 0.27% niobium, 0.10% titanium, 0.05% silicon, 0.01% iron and 0.01% zirconium. Assuming these are lattice impurities, the composition would be 0.30% niobium carbide, 0.13% titanium carbide, 0.07% silicon carbide, 0.01% iron carbide, 0.01% zirconium carbide and 99.48% tantalum carbide. This composition theoretically would contain 6.27% carbon, which was checked reasonably well by actual analysis as 6.24%.

The heat of combustion determinations were conducted with previously described apparatus.² All weights were corrected to vacuum and all heat values are in terms of the defined calorie (1 cal. = 4.1840 abs. joules). The calorimeter was calibrated before each set of measurements by means of benzoic acid (National Bureau of Standards sample 39 g.), the mean value being 32411.1 ($\pm 0.02\%$) cal./ohm.

All combustions were made with 30 atm. oxygen pressure. Ignition of the samples was by means of an electrically heated platinum spiral and a filter paper fuse, for which proper corrections were made. Each substance was tested and found to show no oxidation on standing in the bomb under 30 atm. oxygen pressure before ignition. The bomb gases, after combustion, were tested for oxides of nitrogen. The correction for this was negligible (less than 0.002%) except in the case of zirconium, for which it averaged 0.012% of the heat generated during combustion.

The tantalum combustions employed both plain silica-glass capsules and silica-glass capsules heavily lined with tantalum pentoxide and strongly ignited. In all instances the bomb walls remained entirely clean. No significant difference was noted between the final results with and without the capsule liner, although the combustions were much more nearly complete when no liner was used. Completion of combustion was evaluated for each individual run by means of the observed weight increase of the calorimeter combustion product on prolonged ignition in air. This method showed percentage completion of combustion ranging from 97.23 to 99.99+, and corresponding corrections were applied to the measured heats. (The efficacy of this test was confirmed by experiments with tantalum metal turnings.) X-Ray examination of the combustion product showed it to be the same variety of tantalum pentoxide used previously in low-temperature heat capacity³ and high-temperature heat content⁴ measurements.

The niobium combustions were conducted in silica-glass

(2) G. L. Humphrey, *THIS JOURNAL*, **73**, 1587 (1951).

(3) K. K. Kelley, *ibid.*, **62**, 818 (1940).

(4) R. L. Orr, *ibid.*, **75**, 2808 (1953).